JACS
JOURNAL OF THE AMERICAN CHEMICAL SOCIETY
Communication
pubs.acs.org/JACS

Characterization of an O_2 Adduct of an Active Cobalt-Substituted Extradiol-Cleaving Catechol Dioxygenase

Andrew J. Fielding,[†] John D. Lipscomb,*[,‡] and Lawrence Que, Jr.*[,†]

[†]Department of Chemistry and [‡]Department of Biochemistry, Molecular Biology, and Biophysics and Center for Metals in Biocatalysis, University of Minnesota, Minneapolis, Minnesota 55455, United States

Supporting Information

ABSTRACT: The first example of an O_2 adduct of an active Co-substituted oxygenase has been observed in the extradiol ring cleavage of the electron-poor substrate 4-nitrocatechol (4NC) by Co(II)-homoprotocatechuate 2,3-dioxygenase (Co-HPCD). Upon O_2 binding to the high-spin Co(II) ($S = {}^3/_2$) enzyme–substrate complex, an $S = {}^1/_2$ EPR signal exhibiting ^{59}Co hyperfine splitting (A = 24 G) typical of a low-spin Co(III)–superoxide complex was observed. Both the formation and decay of the new intermediate are very slow in comparison to the analogous steps for turnover of 4NC by native high-spin Fe(II)-HPCD, which is likely to remain high-spin upon O_2 binding. A similar but effectively stable $S = {}^1/_2$ intermediate was formed by the inactive [H200N-Co-HPCD(4NC)] variant. The observations presented shed light on the key roles played by the substrate, the second-sphere His200 residue, and the spin state of the metal center in facilitating O_2 binding and activation.

Homoprotocatechuate 2,3-dioxygenase (HPCD) activates O_2 to carry out the extradiol ring cleavage of homoprotocatechuate (HPCA) (Scheme 1) in the biodegradation

Scheme 1. Extradiol Ring Cleavage of Catechol Substrates by Fe- or Co-Substituted HPCD

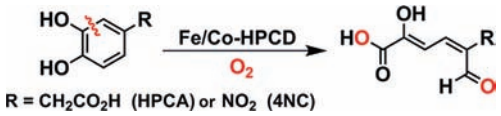

of aromatic compounds by microorganisms.[1−3] Recent metal substitution experiments showed that the native Fe(II) metal cofactor can be substituted with Co(II) to yield Co-HPCD with comparable activity[4] despite an apparent large difference in the M(III/II) redox potentials of Fe-HPCD and Co-HPCD, as suggested by the observation that H_2O_2 oxidatively inactivates Fe-HPCD but not Co-HPCD and the large difference in the standard M(III/II) redox potentials of these metals.[5] As the catalytic mechanism for Fe-HPCD involves O_2 binding to the Fe(II) center,[6−8] our observations raise the question of how O_2 activation and extradiol cleavage can be carried out by the higher-potential Co(II) center of Co-HPCD.

Steady-state kinetics measurements showed Co-HPCD to have a low apparent O_2 affinity ($K_M^{O_2}$ = 1.2 ± 0.1 mM vs 60 μM for Fe-HPCD at pH 7.8), perhaps reflecting the higher potential of the Co(II) center. However, under O_2-saturating conditions, Co-HPCD shows a higher HPCA ring cleavage activity than Fe-HPCD (k_{cat} = 1120 ± 70 min^{-1} vs 470 ± 20 min^{-1} for Fe-HPCD at pH 7.8).[4] Comparisons of transient kinetic experiments indicated different rate-limiting steps for the Fe-HPCD- and Co-HPCD-catalyzed reactions. Whereas the rate-limiting step for Fe-HPCD occurs in the product release phase of the catalytic cycle,[6,9,10] that for Co-HPCD occurs in the O_2 binding and activation phase of the reaction. Investigation of these steps has been facilitated in our past studies of extradiol dioxygenases by the use of the slow substrate analogue 4-nitrocatechol (4NC).[6,9,10] This electron-poor substrate is cleaved at the same position as HPCA by Co-HPCD, but the rate of the reaction is decreased 1000-fold (pH 6.0, 22 °C, 2 atm O_2). This has allowed us to trap an O_2 adduct and characterize it as a low-spin Co(III)–superoxide complex, the first documented example of such a species for a functional cobalt oxygenase.

Co-HPCD binds 4NC [K_D^{4NC} = 5 ± 2 μM; Figure S1 in the Supporting Information (SI)] in its purple dianionic form with an intense absorption band at 516 nm that slowly converts to the yellow extradiol ring-cleaved product with absorption bands at 330 and 390 nm at pH 6.0 (Figure 1).[9] Time-dependent traces of the reaction at 516 and 390 nm were fit satisfactorily with single-exponential equations to give nearly the same $1/\tau$ value at these two wavelengths (Figure S2). The conversion exhibited a linear dependence on O_2 concentration (Figure 1 inset), suggesting that O_2 binding is the first and rate-limiting step over the experimentally accessible [O_2] range. The slope of the plot gave a second-order rate constant for O_2 binding of 30 ± 3 M^{-1} min^{-1}, which is at least 6 orders of magnitude smaller than that for O_2 binding to [Fe-HPCD(4NC)].[9,10] This is in accord with our previous proposal, based on steady-state kinetic analysis, that the O_2 binding step in HPCA turnover by Co-HPCD is slow and rate-limiting.[4] Because of the slow turnover of 4NC by Co-HPCD, the observed activity could originate from contaminating Fe-HPCD. To rule out this possibility, the enzyme was pretreated with H_2O_2 to inactivate any contaminating Fe-HPCD.[11] Furthermore, in the single turnover of 4NC by Fe-HPCD, none of the observed kinetic phases show an O_2 concentration dependence, in contrast to our observations here for Co-HPCD (Figure 1 inset and Figure S2).[9]

Electron paramagnetic resonance (EPR) freeze–quench experiments were performed by rapidly mixing the anaerobic [Co-HPCD(4NC)] complex (pH 6 at 22 °C) with O_2-saturated

Received: October 10, 2011
Published: December 16, 2011

   dx.doi.org/10.1021/ja2095365 | J. Am. Chem.Soc. 2012, 134, 796–799

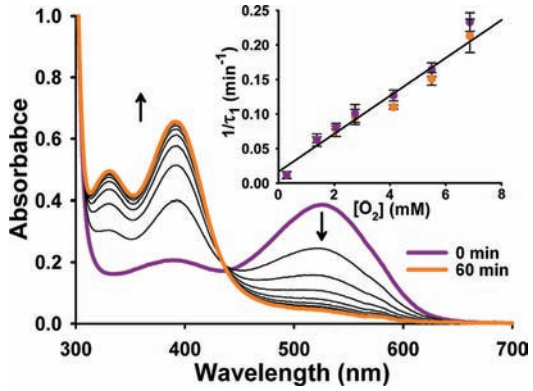

Figure 1. UV−vis absorption spectra observed for the single-turnover reaction of O_2 with [Co-HPCD(4NC)] (40 μM 4NC and 150 μM Co-HPCD) (purple) to form the extradiol ring-cleaved product (orange). Reaction conditions: 50 mM MES (pH 6.0), 2 atm O_2, 22 °C. Intermediate lines were obtained at 5 min intervals. Inset: O_2 dependence of average $1/\tau$ values from single-exponential fits of data (Figure S2) at either 516 (purple points) or 390 nm (orange points). The thin black line represents a linear fit of the $1/\tau$ data points.

buffer and then placing the reaction under 2 atm O_2. Aliquots from the reaction were then taken every few minutes over the course of 60 min and frozen in EPR tubes. Figure 2 shows representative EPR

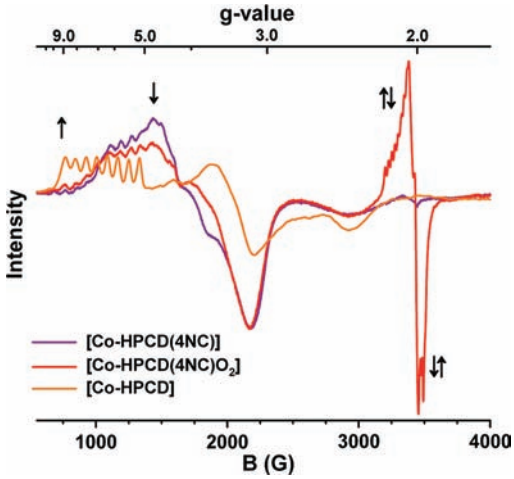

Figure 2. EPR spectra of freeze−quench samples of anaerobic enzyme−substrate complex [Co-HPCD(4NC)] (purple) rapidly mixed with O_2-saturated buffer under 2 atm O_2 at 22 °C in 50 mM MES buffer (pH 6.0), showing formation of the [Co-HPCD(4NC)O_2] intermediate (red) at 2 min and subsequent decay to Co-HPCD (orange) and the extradiol ring-cleaved product after 60 min. The initial concentrations of reactants were 0.5 mM [Co-HPCD(4NC)] and 2.75 mM O_2.

spectra from the freeze−quench experiments. Co-HPCD exhibited an $S = {}^3/_2$ EPR signal associated with a high-spin Co(II) center (Figure S3),[4] with the signal at $g = 6.7$ showing ^{59}Co ($I = {}^7/_2$) hyperfine splitting ($A = 80$ G) (Table 1). The $S = {}^3/_2$ signal changed upon anaerobic formation of the [Co-HPCD(4NC)] complex (Figure 2 and Figure S3). Upon mixing with O_2, the amount of the $S = {}^3/_2$ species decreased, as indicated by a decrease in the feature at $g = 4.8$, and a new $S = {}^1/_2$ species formed with signals centered at $g = 2$. The new $S = {}^1/_2$ species exhibited well-resolved eight-line hyperfine splitting from the ^{59}Co nucleus ($A = 24$ G). The intensity of the $S = {}^1/_2$ species continued to increase

Table 1. EPR Data for Co(II)-HPCD Complexes

sample	S	g values	$A_x(^{59}\text{Co})$
Co-HPCD[a]	$^3/_2$	6.7, 3.4, 2.4	80 G
[Co-HPCD(HPCA)][a]	$^3/_2$	7.6, 2.5, 1.9	98 G
[Co-HPCD(4NC)][b]	$^3/_2$	5.6, 3.5, 2.1	75 G
[Co-HPCD(4NC)O_2]	$^1/_2$	2.10, 2.02, 1.99	24 G
[H200N-Co-HPCD][b]	$^3/_2$	6.9, 3.7, 2.6	90 G
[H200N-Co-HPCD(4NC)][b]	$^3/_2$	6.3, 3.2, 1.9	53 G
[H200N-Co-HPCD(4NC)O_2]	$^1/_2$	2.10, 2.02, 1.99	22 G

[a]Reference 4. [b]Figure S3.

over the first 2 min and then decreased as the $S = {}^3/_2$ signal of Co-HPCD at $g = 8.9$ grew.

The reaction progress (Figure 3) was monitored by following changes in the intensities of EPR features unique to each

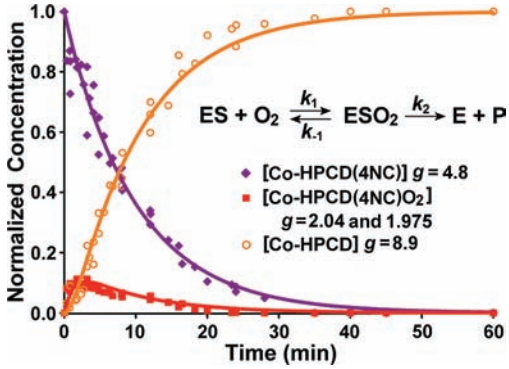

Figure 3. Time dependences of the various EPR-active species observed in the EPR freeze−quench experiments. The change in concentration of each species was measured by monitoring the change in the intensity of EPR features unique to that species. The initial and final spectra were used to normalize the concentrations of [Co-HPCD(4NC)] and Co-HPCD, respectively. The maximum yield of [Co-HPCD(4NC)O_2] was measured by spin quantification and used to normalize its concentration.[12] Solid lines represent fits of data by global analysis to rate equations based on the reaction scheme shown in the inset.

species. A yield of ~10% for the $S = {}^1/_2$ species was measured at 2 min by spin quantification.[12] The ability to observe the intermediate directly allowed accurate fitting of the time course to the appropriate equation for a two-step reaction. The EPR and UV−vis reaction progress curves (Figure 3 and Figure S4) were fit simultaneously by global analysis to rate equations based on the reaction scheme shown in Figure 3 using the program DYNAFIT, and the following rate constants were obtained: $k_1 = 40 \pm 5$ M^{-1} min^{-1}, $k_{-1} = 0.05 \pm 0.01$ min^{-1}, and $k_2 = 0.72 \pm 0.06$ min^{-1}.[13] Under this model, the $k_1[O_2]$ and k_2 values are comparable in magnitude, with $k_1[O_2] < k_2$ at experimentally accessible O_2 pressures (<5 atm). The ~10% yield of the $S = {}^1/_2$ species observed in the freeze−quench EPR experiments at 2 atm O_2 is fully consistent with the rate constants obtained.

The H200N-Co-HPCD mutant showed no extradiol ring-cleavage activity for 4NC at any of the pHs examined. Nevertheless, the [H200N-Co-HPCD(4NC)] complex could form an O_2 adduct with an $S = {}^1/_2$ EPR spectrum similar to that of [Co-HPCD(4NC)O_2] (Figure 4). In fact, because $k_2 = 0$, the intermediate was formed in higher yield (50% under 2 atm O_2), facilitating investigation of its properties. Interestingly, no significant UV−vis spectral changes between [H200N-Co-HPCD(4NC)] and [H200N-Co-HPCD(4NC)O_2] were

dx.doi.org/10.1021/ja2095365 | J. Am. Chem.Soc. 2012, 134, 796−799

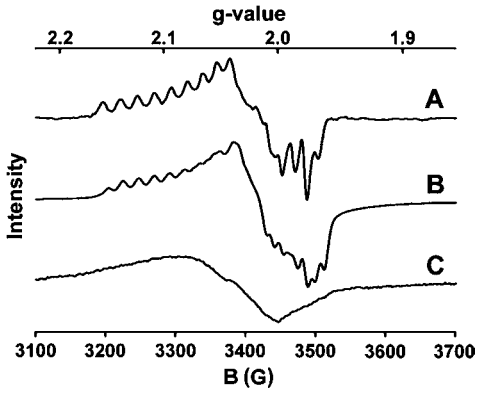

Figure 4. EPR spectra of (A) [Co-HPCD(4NC)$^{16}O_2$] at pH 6.0, (B) [H200N-Co-HPCD(4NC)$^{16}O_2$] at pH 7.5, and (C) [H200N-Co-HPCD(4NC)$^{17}O_2$] at pH 7.5 (prepared with 70% $^{17}O_2$). Spectra were obtained at 9.64 GHz using a microwave power of 20 dB at 20 K.

observed (Figure S5), suggesting that the 4NC chromophore is not affected by O_2 binding. Accordingly, O_2 binding to [H200N-Co-HPCD(4NC)] proved to be reversible, as purging the sample with argon caused the $S = {}^1/_2$ species to disappear, restoring the EPR signal of the enzyme–substrate (ES) complex (Figure S6). O_2 binding experiments monitored by EPR spectroscopy (Figure S7) showed that [H200N-Co-HPCD(4NC)] has a low affinity for O_2, with a $K_D^{O_2}$ of 2.8 ± 0.2 mM O_2 at pH 7.5, similar to the value of 1.3 mM O_2 deduced for Co-HPCD from the kinetic fits described above.

Both the H200N and wild-type [Co-HPCD(4NC)O_2] adducts exhibited small ^{59}Co hyperfine splittings of <25 G (Table 1). These are comparable to those of other characterized low-spin Co(III)–superoxide species (Table S1), where the unpaired electron is localized on the superoxide moiety and the observed ^{59}Co hyperfine splitting is attributed to spin polarization.[14−16] Furthermore, the use of $^{17}O_2$ ($I = {}^5/_2$) resulted in significant broadening of the $S = {}^1/_2$ EPR signals of both the H200N and wild-type [Co-HPCD(4NC)O_2] adducts (Figure 4C and Figure S8), in strong support of the low-spin Co(III)–superoxo description for the adducts.

The binding of O_2 to the ES complex of Co-HPCD results in an apparent spin state change from high-spin Co(II) in the ES complex to low-spin Co(III) in the O_2 adduct. However, as expected, such a spin transition is not observed for the corresponding O_2 adducts of Fe- or Mn-HPCD because of the weak-field nature of the HPCD coordination environment.[6,17] Co(III) differs from the other two metal centers because of its d^6 electron configuration and the consequent large ligand-field stabilization energy that favors the low-spin state, as found for all Co(III)–superoxide complexes characterized to date.[15,16] The formation of the low-spin adduct is likely to be an important factor that promotes O_2 binding despite the high Co(III/II) potential. However, the required reorganization that accompanies the spin transition as the O_2 adduct forms and the high Co(III/II) potential work together to raise the barrier for O_2 binding, which shifts the rate-limiting step to the O_2-binding phase of the catalytic cycle for Co-HPCD.[4]

The decay rate of the observed low-spin Co(III)–superoxide species is at least 7 orders of magnitude lower than the rate of the analogous step using Fe-HPCD,[9,10] even though one may expect Co(III) to be a stronger oxidant than Fe(III) in the subsequent one-electron oxidation of 4NC. This slow rate of 4NC oxidation likely reflects the large kinetic barrier arising from an increase in the reorganization energy upon electron transfer as the low-spin Co(III)–superoxide converts to a high-spin Co(II)(semiquinone)–superoxide species (Scheme 2).[18]

Scheme 2. Proposed O_2 Activation Mechanism by Co-HPCD with HPCA at pH 9.0 and 4NC at pH 5.5[4]

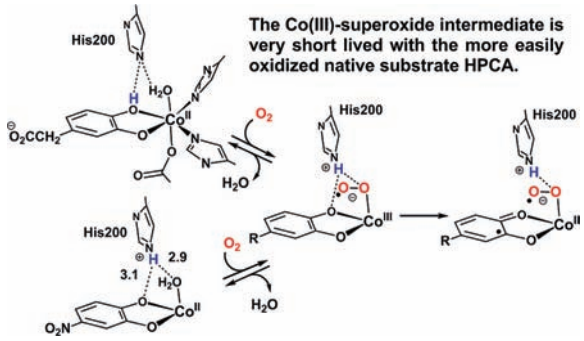

His200 has been shown previously by site-directed mutagenesis to be a catalytically important residue for Fe-HPCD.[6,10,19,20] The fact that H200N-Co-HPCD is not catalytically active but is nonetheless able to bind O_2 reversibly when 4NC is bound to the cobalt center suggests that the H200 residue is not required for O_2 binding but must be essential for a subsequent step. In Fe-HPCD crystal structures of the substrate complex and intermediates following O_2 binding, H200 is observed to be involved in weak hydrogen-bonding interactions with the OH moiety of the monoanionically bound catecholate as well as stronger interactions with the various O_2-derived ligands.[7,21−23] His200 has been proposed to facilitate electron transfer from the substrate to the M–O_2 unit by a proton-coupled electron transfer mechanism, where it acts as a base to remove the proton from the substrate to assist in catechol oxidation. In turn, the protonated His200 residue can interact with the O_2 adduct as it forms and stabilize the developing negative charge on the dioxygen moiety.[7,21] In the next step, the protonated His200 may also help to orient the superoxide moiety to optimize its attack on the substrate semiquinone radical to form the alkylperoxo intermediate that leads to the extradiol cleavage of the substrate.[6,7] These proposed roles are illustrated in Scheme 2.

Scheme 2 can also rationalize the dramatically different pH–activity profiles of Co-HPCD with HPCA and 4NC as substrates. Optimal extradiol cleavage of HPCA occurs at pH 9.0 (Figure S9), but for 4NC the optimum pH is 5.5 (Figure S10). This may arise from the drastically different pK_a's of HPCA and 4NC,[24,25] resulting in HPCA binding to Co-HPCD as a monoanionic catecholate and 4NC binding as a dianion.[9,26,27] In the latter case, the intensity of the characteristic 516 nm band of the dianion decreases and the rate of 4NC turnover increases as the pH is lowered (Figures S10 and S11A). However, the decrease in the 516 nm band is not accompanied by the appearance of a 425 nm chromophore associated with the 4NC monoanion (Figure S11A),[26,27] so lowering the pH from 9.0 to 5.5 does not result in protonation of the bound 4NC. Instead, we suggest that H200 becomes protonated and then hydrogen-bonds to the bound 4NC to affect its chromophore. This notion is consistent with the observation that the 4NC chromophore of the [H200N-Co-HPCD(4NC)] complex is much less sensitive to changes in pH (Figure S11B). As Asn200 has a shorter side chain and cannot be protonated in this pH range, it is unable to interact productively

dx.doi.org/10.1021/ja2095365 | J. Am. Chem.Soc. 2012, 134, 796−799

with 4NC. The differences in the pH−activity profiles for HPCA and 4NC as substrates can thus be rationalized by the key role proposed for H200 as an acid/base catalyst to promote electron transfer from the substrate to the M−O_2 unit to advance the reaction cycle beyond the O_2 binding step. In the case of HPCA, protonation of H200 occurs upon extraction of the proton from the bound substrate concomitant with its oxidation. The analogous proton transfer to H200 cannot occur for 4NC, as it is bound as a dianion. However, H200 can be protonated by solvent at lower pH, resulting in the observed increase in the rate of 4NC cleavage (Figure S10). The H200N mutation prevents the ring cleavage reaction by eliminating both protonation pathways as well as any effects on orientation of the oxy moiety.

The H200N-Fe-HPCD, mutant is similarly unable to catalyze extradiol cleavage of 4NC but instead catalyzes the two-electron oxidation of 4NC to yield quinone and H_2O_2.[6,9,10] Initial O_2 binding to [H200N-Fe-HPCD(4NC)] is very rapid and reversible ($k_1 = 9 \pm 1.2 \times 10^6$ M^{-1} min^{-1} and $k_{-1} = 3120$ min^{-1} at 4 °C and pH 7.5) and leads to the formation of a long-lived Fe(III)−superoxo species analogous to the Co(III)−superoxo species observed in this study. This shows that the initial electron transfer step from M(II) to O_2 proceeds with either metal in the absence of H200. However, the subsequent electron transfer step from substrate to the M−O_2 unit is clearly blocked for the unreactive low-spin [H200N-Co-HPCD(4NC)O_2] species but can still occur for the high-spin [H200N-Fe-HPCD(4NC)O_2] intermediate (k = 1.32 min^{-1} at 4 °C and pH 7.5) to form a high-spin Fe(III)−(4-nitrobenzosemiquinone)peroxo intermediate.[6,10]

In summary, we have characterized the O_2 adduct of a cobalt-substituted iron dioxygenase that exhibits activity comparable to that of its iron analogue. The O_2 adduct is best described as a low-spin Co(III)−superoxo complex,[14−16] the first example of such a species for a functional cobalt oxygenase. We have also shown that H200 plays a crucial role in promoting the subsequent oxidation steps that lead to extradiol cleavage of the substrate by acting as an acid/base catalyst and properly orienting the superoxide to attack the substrate. The substitution of Co(II) for the native Fe(II) center in HPCD shifts the rate-limiting step from the product release phase of the catalytic cycle in the case of the Fe(II) enzyme to the O_2 binding and catechol oxidation phase for the Co(II) enzyme.[9,10] This shift probably results from the higher kinetic barrier associated with O_2 binding to Co-HPCD due to the higher M(III/II) redox potential of the cobalt center and the spin transition from high-spin Co(II) to low-spin Co(III) upon O_2 binding to Co-HPCD. It may also involve the reverse spin transition in the subsequent electron transfer from the electron-poor 4NC substrate to the low-spin Co−superoxo unit. A similar change in the oxidation and spin state presumably occurs as [Co-HPCD(HPCA)] binds O_2, but this remains to be demonstrated. However, the fact that the HPCA reaction is at least 1000-fold faster than that for 4NC suggests that the lifetime of the putative low-spin Co(III)−superoxo intermediate significantly decreases as the electron-poor 4NC is replaced with the more easily oxidized substrate. Further efforts are aimed at trapping the analogous superoxo intermediate with substrates other than 4NC.

■ ASSOCIATED CONTENT

Supporting Information

Experimental procedures and supporting figures. This material is available free of charge via the Internet at http://pubs.acs.org.

■ AUTHOR INFORMATION

Corresponding Author

lipsc001@umn.edu; larryque@umn.edu

■ ACKNOWLEDGMENTS

This work was supported by NIH Grants GM 24689 to J.D.L. and GM 33162 to L.Q. A.J.F. thanks the University of Minnesota Chemical Biology Initiative for financial support in conjunction with the NIH-supported Chemistry Biology Interface Training Grant (GM 08700). We thank Michael Mbughuni for providing the $^{17}O_2$-saturated buffer solutions for the EPR experiments.

■ REFERENCES

(1) Smith, M. R. *Biodegradation* **1990**, *1*, 191.
(2) Orville, A. M.; Lipscomb, J. D. *Met. Ions Biol. Syst.* **1992**, *28*, 243.
(3) Miller, M. A.; Lipscomb, J. D. *J. Biol. Chem.* **1996**, *271*, 5524.
(4) Fielding, A. J.; Kovaleva, E. G.; Farquhar, E. R.; Lipscomb, J. D.; Que, L. Jr. *J. Biol. Inorg. Chem.* **2011**, *16*, 341.
(5) Bratsch, S. G. *J. Phys. Chem. Ref. Data* **1989**, *18*, 1.
(6) Mbughuni, M. M.; Chakrabarti, M.; Hayden, J. A.; Bominaar, E. L.; Hendrich, M. P.; Münck, E.; Lipscomb, J. D. *Proc. Natl. Acad. Sci. U.S.A.* **2010**, *107*, 16788.
(7) Kovaleva, E. G.; Lipscomb, J. D. *Science* **2007**, *316*, 453.
(8) Mbughuni, M. M.; Chakrabarti, M.; Hayden, J. A.; Meier, K. K.; Dalluge, J. J.; Hendrich, M. P.; Münck, E.; Lipscomb, J. D. *Biochemistry* **2011**, *50*, 10262.
(9) Groce, S. L.; Miller-Rodeberg, M. A.; Lipscomb, J. D. *Biochemistry* **2004**, *43*, 15141.
(10) Groce, S. L.; Lipscomb, J. D. *Biochemistry* **2005**, *44*, 7175.
(11) Emerson, J. P.; Kovaleva, E. G.; Farquhar, E. R.; Lipscomb, J. D.; Que, L. Jr. *Proc. Natl. Acad. Sci. U.S.A.* **2008**, *105*, 7347.
(12) Aasa, R.; Vänngård, T. *J. Magn. Reson.* **1975**, *19*, 308.
(13) Kuzumic, P. *Anal. Biochem.* **1996**, *237*, 260.
(14) (a) Niswander, R. H.; Taylor, L. T. *J. Magn. Reson.* **1977**, *26*, 491. (b) Hoffman, B. M.; Damon, L. D.; Basolo, F. *J. Am. Chem. Soc.* **1970**, *92*, 61. (c) Tovrog, B. S.; Kitko, D. J.; Drago, R. S. *J. Am. Chem. Soc.* **1976**, *98*, 5144.
(15) Smith, T. D.; Pilbrow, J. R. *Coord. Chem. Rev.* **1981**, *39*, 295.
(16) Jones, R. D.; Summerville, D. A.; Basolo, F. *Chem. Rev.* **1979**, *79*, 139.
(17) Gunderson, W. A.; Zatsman, A. I.; Emerson, J. P.; Farquhar, E. R.; Que, L. Jr.; Lipscomb, J. D.; Hendrich, M. P. *J. Am. Chem. Soc.* **2008**, *130*, 14465.
(18) Basolo, F.; Pearson, R. G. *Mechanisms of Inorganic Reactions: A Study of Metal Complexes in Solution*, 2nd ed.; Wiley: New York, 1967; Chapter 6.
(19) Emerson, J. P.; Wagner, M. L.; Reynolds, M. F.; Que, L. Jr.; Sadowsky, M. J.; Wackett, L. P. *J. Biol. Inorg. Chem.* **2005**, *10*, 751.
(20) Groce, S. L.; Lipscomb, J. D. *J. Am. Chem. Soc.* **2003**, *125*, 11780.
(21) Vetting, M. W.; Wackett, L. P.; Que, L. Jr.; Lipscomb, J. D.; Ohlendorf, D. H. *J. Bacteriol.* **2004**, *186*, 1945.
(22) Davis, M. I.; Wasinger, E. C.; Decker, A.; Pau, M. Y. M.; Vaillancourt, H. F.; Bolin, J. T.; Eltis, L. D.; Hedman, B.; Hodgson, K. O.; Solomon, E. I. *J. Am. Chem. Soc.* **2003**, *125*, 11214.
(23) Vaillancourt, F. H.; Barbosa, C. J.; Spiro, T. G.; Bolin, J. T.; Blades, M. W.; Turner, R. F. B.; Eltis, L. D. *J. Am. Chem. Soc.* **2002**, *124*, 2485.
(24) Cornard, J.-P.; Rasmiwetti.; Merlin, J.-C. *Chem. Phys.* **2005**, *309*, 239.
(25) Perrin, D. D.; Dempsey, B.; Serjeant, E. P. *pK_a Prediction for Organic Acids and Bases*; Chapman and Hall: London, 1981.
(26) Tyson, C. *J. Biol. Chem.* **1975**, *5*, 1765.
(27) Reynolds, M. F.; Costas, M.; Ito, M.; Jo, D.-H.; Tipton, A. A.; Whiting, A. K.; Que, L. Jr. *J. Biol. Inorg. Chem.* **2003**, *8*, 263.